RSC Advances

ROYAL SOCIETY OF CHEMISTRY

www.rsc.org/advances

Effect of Hydrothermal Treatment Time and Carbon Coating Amount on Performance of PtRu/C Catalyst for Direct Methanol Fuel Cell

Cun-Zhi Li [a,b] ,Zhen-Bo Wang [a,c]*, Jing Liu [d],

Chun-Tao Liu [d], Da-Ming Gu [b], Jie-Cai Han [c]

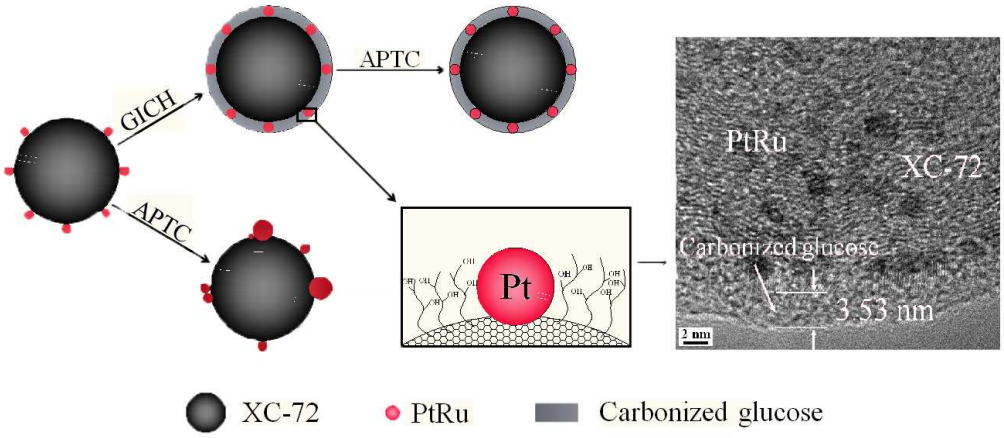

The mean size of the as-prepared metal nanoparticles grew remarkable because of the coalescence by its migration on the support surface during the accelerated potential cycling test. However, that of the carbon riveted metal nanoparticles grew slightly, which is because the existence of carbon nanolayer (about 3.5 nm from HTEM) on the surface of the support from glucose in-situ carbonization inhibits the migration and coalescence of PtRu nanoparticles on the support. The APTC and the life test of single cells indicate that the stability of carbon riveted PtRu/C catalyst is

about double time than that of the as-prepared PtRu/C with the similar activity.

Effect of hydrothermal treatment time and carbon coating amount on performance of PtRu/C catalysts for direct methanol fuel cell

Cun-Zhi Li [a,b] ,Zhen-Bo Wang [a,c]*, Jing Liu [d], Chun-Tao Liu [d], Da-Ming Gu [b], Jie-Cai Han [c]

[a] School of Chemical Engineering and Technology, Harbin Institute of Technology, No.92 West-Da Zhi Street, Harbin, 150001 China

[b] School of Science, Harbin Institute of Technology, No.92 West-Da Zhi Street, Harbin, 150001 China

[c] School of Materials Science and Engineering, Harbin Institute of Technology, No.92 West-Da Zhi Street, Harbin, 150001 China

[d] School of Chemistry and Materials Science, Heilongjiang University, No. 74 Xue-Fu Road, Harbin 150080, China

[*] *Corresponding author. Tel.: +86-451-86417853; Fax: +86-451-86418616*

E-mail address: wangzhb@hit.edu.cn (Z.B. Wang)

Abstract

High stable carbon riveted PtRu/C catalyst has been synthesized through glucose in-situ carbonization by hydrothermal method (GICH). Its inner mechanism and practical application are further researched by X-ray diffraction, high resolution transmission electron microscopy, X-ray photoelectron spectroscopic, single fuel cell test, and conventional electrochemical measurements. The single fuel cell test demonstrates that the GICH method has the bright application value. After 100 h life test, the maximum power density of single cell used carbon riveted PtRu/C as anode catalyst drops only 12.0% from 76.6 to 67.4 mW cm^{-2}, comparing the 28.4% from 73.2 to 52.4 mW cm^{-2} for as-prepared PtRu/C. In addition, when the optimal

hydrothermal treatment time is 4 h and the carbon coating amount is 9%, the carbon riveted PtRu/C catalyst coated by 3.5 nm carbon layer has the best stability with a similar initial activity compared to as-prepared PtRu/C. The significantly enhanced stability of carbon riveted PtRu/C is attributed to two critical reasons: (1) the anchoring effect of glucose carbon nanolayer formed during the glucose in-situ carbonization through hydrothermal method; (2) the content increasing of Pt (0), Ru(0), sp^3 hybridization carbon and C-OR groups composition and the evidently decreasing PtO_2 and RuO_xH_y after the carbon riveted process.

Keywords: direct methanol fuel cell, stability, life test, carbon riveted, carbon supported PtRu alloy catalyst, methanol oxidation

1. Introduction

Compared with hydrogen proton exchange membrane fuel cells (PEMFCs), direct methanol fuel cells (DMFCs) with renewable liquid methanol as fuel have a unique advantage because methanol is safe for storage and transportation.[1-4] During methanol oxidation, pure platinum is poisoned by the adsorption of CO as an intermediate. The addition of ruthenium to platinum improves the rate of methanol oxidation via the bifunctional mechanism.[5] However, the stability of PtRu/C catalyst continues to stifle their commercialization of those systems for stationary and transportation power applications.

To improve the durability of catalysts for DMFCs or PEMFCs, extensive researches have been carried out through variety methods. Some researchers focus on the preparation of Pt based alloys[6] or modification by other metals. For example, Pt–M (M = Cu, Co, Ni, Fe) nanowires show more superior activity and stability than the corresponding pure Pt nanowires and Pt black.[7] After 1000 cycling the potential between 0.2 and 1.0 V with a scan rate of 200 mV s^{-1} in 1.0 mol L^{-1} CH_3OH and 0.5 mol L^{-1} H_2SO_4 solution, the current densities of the

peaks for the commercial Pt black and Pt nanowires drop dramatically with the initial activity of 0.20 and 0.47 A mg_{pt}^{-1}, respectively. However, the current densities of Pt-M nanowires dropped less upon cycling with the initial activity of 0.89, 0.82, 0.87 and 0.79 A mg_{pt}^{-1} for Pt-Cu, Pt-Ni, Pt-Co and Pt-Fe respectively. The second approach is modification of the catalyst supports. A variety of carbon based materials[8] such as carbon nanotubes (CNT)[9-12], carbon nanofibers (CNF)[13], and graphene[14-16] as well as non-carbonaceous based materials, e.g. titania[17, 18], indium oxides[19], silica[20], tungsten oxide[21-23], manganese dioxide[24] and g-C_3N_4[25-27] are attractive candidates for the catalyst support. Zhang and co-workers[28] synthesized and studied 3D ordered mesoporous carbon sphere array (OMCS)-supported Pt nanoparticles (Pt/OMCS). After 1000 cycling the electrode potential between 0 and 1.3 V at a scan rate of 50 mV s^{-1} in argon-purged 0.5 mol L^{-1} H_2SO_4 solution at room temperature, the Pt/OMCS catalyst loses only 26% of its Pt ECSA after 1000 cycles, whereas that of the Pt/XC-72R and commercial Pt/C catalysts has decreased by 46% and 64%, respectively. And their initial mass activities are 0.671, 0.118 and 0.145 A mg_{pt}^{-1} for Pt/OMCS, Pt/XC-72R and commercial Pt/C respectively. Besides, there were also some reports focused on migration and coalescence of metal particles by coating a porous shell such as SiO_2[29], TiO_2[30], and polybenzimidazole derivatives (PBIs)[31] on the catalyst surface. Zhou and co-workers[32] studied the stability of PtRu/CNT coated with MnO_2 catalyst. After 2000 potential cycles in 1 mol L^{-1} $HClO_4$ with 1 mol L^{-1} CH_3OH, 55% and 30% activity remained with the initial activity of 0.48 and 0.44 A mg_{Pt}^{-1} for MnO_2/PtRu/CNT and PtRu/CNT catalyst, respectively.

In our previous work[33-36], we have reported a method to enhance the stability of PtRu/C catalyst by in situ carbonization of glucose. Many high stable catalysts were designed and prepared, such as Pt/C, Pt/TiO_2-C, Pt/MWCNTs-TiO_2, Pt/MWCNTs–Al_2O_3, and so on. However, this method needs a high temperature of 400°C, which leads to remarkable increasing of Pt nanoparticles. In addition, the pyknotic carbonized carbon nanolayer formed

through thermal method could cover some Pt active sites. To solve this problem, the carbon riveted PtRu/C catalysts have been prepared through hydrothermal method.[37] However, that work is quality incomplete. We don't have a thorough knowledge of the carbonized carbon on surface of the catalyst, such as its morphology and functions. While, the effect of hydrothermal treatment time and carbon coating amount on performance of PtRu/C catalysts also should be further studied. In this work, we first confirm the carbonized carbon layer about 2-5 nm is successfully coated on the surface of as-prepared PtRu/C catalyst. The nanolayers from glucose in-situ carbonization can greatly inhibit the migration and coalescence of PtRu nanoparticles on the support. Furthermore, the practical application value of this method is also proved by single fuel cell life test. After 100 h life test, the maximum power density of single cell used carbon riveted PtRu/C catalyst drops only 12.0%, comparing the 28.4% from for as-prepared PtRu/C.

2. Experimental

2.1 Catalysts preparation

In present work, all chemicals were analytical reagent. Hexachloroplatinic acid ($H_2PtCl_6 \cdot 6H_2O$) and ruthenium chloride ($RuCl_3$) were purchased from General Research Institute for Nonferrous Metals, Beijing, China. Vulcan XC-72 carbon black with mean particle size of about 20 nm was purchased from Cabot and 5 wt. % Nafion® solutions were obtained from Dupont. The PtRu/C (metal loading of 20 wt. % supported XC-72R, Cabot) catalyst was prepared through a microwave-assisted polyol process (MAPP) [22, 23] and the atomic ratio of Pt/Ru was adjusted to that of the commercial catalyst (atomic ratio of 1:1). Briefly, Vulcan XC-72 carbon black of 50 mg was dispersed into the mixed solution of 30 mL containing ethylene glycol (EG) and isopropyl alcohol (V/V = 4:1) in 100 ml beaker under ultrasonic treatment for 1 h to form uniform carbon ink, then 0.0378 mol L^{-1} H_2PtCl_6-EG of 1.2 ml and 0.02 mol L^{-1} $RuCl_3$-EG of 2.2 ml with the subsequent mixing process for 3 h.

Followed by adjusting the pH (pHS-32 meter) to 8 by using a 1 mol L^{-1} NaOH ethylene alcohol solution, the suspension was subjected to consecutive microwave heating for 50 s in a microwave oven (from Galanz Ltd., 800 W) under flowing Ar. After the solution was cooled to room temperature, its pH value was adjusted to 2 by HNO_3 aqueous solution, which was then stirred for 12 h. Finally, the product was filtered, washed several times with ultrapure water (Millipore, 18.2 MΩ·cm). The obtained PtRu/C catalyst was dried for 3 h at 80 ^oC and then stored in a vacuum vessel.

The as-prepared PtRu/C was riveted by carbon nanolayer forming glucose in-situ carbonization through hydrothermal method. In brief, 50mg as-prepared PtRu/C and a calculated amount of glucose (6% mass ratio of carbonized carbon from the carbonization of glucose to the PtRu/C catalyst) were dispersed into 250 mL ultrapure water in a beaker under ultrasonic treatment for 1 h. Then, the mixed suspension was transferred into a reaction kettle (CJF-1L, from Reflection Axe Industry Factory of China Dalian) and argon gas was fed into the ink for 15 min to remove oxygen for consecutive hydrothermal at 160^oC for several hours. After it was cooled to room temperature, the carbon riveted PtRu/C catalyst was washed, dried, and stored in vacuum.

The 40 wt. % Pt/C and 40 wt. % PtRu/C catalysts used for single fuel cell were prepared in the similar way. The coating amount of carbon riveted 40 wt. % PtRu/C is 9%, and the hydrothermal treatment time is 4 h.

2.2 MEA preparation

The as-prepared and the carbon riveted 40 wt. % PtRu/C were compared as the different anode catalysts to fabricate single fuel cell. And the cathode catalyst was the homemade 40 wt. % Pt/C. PtRu/C and 5 wt. % Nafion® ionomer solution (DuPont Co., EW=1100) were mixed in isopropanol alcohol solution to form a homogeneous catalyst suspension for the anode. The cathodic catalyst ink was prepared similarly with Pt/C, Nafion® ionomer, and

PTFE latex. The Nafion® contents in both anodic and cathodic catalyst layers were 20 wt. %. The catalyst inks were deposited onto the gas diffusion layers (GDLs) by paint brush with a metal loading of 2.5 mg cm^{-2} for both electrodes. The anode and cathode GDL were both prepared by using spray painting method with a carbon black of 1 mg cm^{-2} and 5% Nafion® ionomer solution on the carbon paper (Toray paper TGPH 090). DuPont Nafion® 117 membrane was used as the solid electrolyte. Before being applied to the electrodes, the Nafion® membrane was pretreated by sequential immersion in boiling solution of 3 wt. % H_2O_2 solutions, ultrapure water, boiling solution of 0.5 mol L^{-1} H_2SO_4, and ultrapure water, where each step lasted 1 h. The pretreated Nafion® membranes sandwiched between the anode electrodes and the cathode electrodes and then the assemblies were hot pressed under a specific loading of 100 kg cm^{-2} for 1.5 min at 135°C.

2.3 Physical characterization

2.3.1. X-ray diffraction (XRD)

The D/max-RB diffractometer (made in Japan) using a Cu K*a* X-ray source operating at 45 kV and 100 mA, scanning at a rate of 4 ° min^{-1} with an angular resolution of 0.05º was used to obtain the XRD patterns of all catalysts.

2.3.2. Transmission electron microscopy (TEM) and high resolution transmission electron microscopy (HRTEM)

TEM, HRTEM images of all catalysts were characterized by using a TECNAI G2 F30 field emission transmission electron microscope with a spatial resolution of 0.17 nm. Before taking the electron micrographs, the samples were prepared by ultrasonically dispersing the catalyst powder in ethanol. A drop of the suspension was deposited on a standard copper grid coated with carbon film. The copper grid was then dried overnight. The applied voltage was 300 kV.

2.3.3. X-ray photoelectron spectroscopy (XPS)

To determine the surface properties of the catalysts, XPS analysis was carried out by using the Physical Electronics PHI model 5700 instrument. Before XPS analysis, all samples were dried in vacuum at 80 ^{o}C overnight. The take-off angle of the sample to analyzer was 45^{o} and the Al X-ray source was operated at 250 W. Survey spectra were collected at a pass energy (PE) of 187.85 eV over a binding energy range from 0 eV to 1300 eV. High binding energy resolution multiplex data for the individual elements were collected at a PE of 29.55 eV. During all XPS experiments, the pressure inside the vacuum system was maintained at 1×10^{-9} Pa.

2.4 Electrochemical measurements

Electrochemical measurements were performed by using a CHI 650D potentiostat and a conventional three-electrode electrochemical cell. The counter electrode was Pt sheet of 1 cm^2 plate and Hg/Hg_2SO_4 electrode (–0.68 V relative to reversible hydrogen electrode, RHE) was used as the reference electrode. The as-prepared PtRu/C and carbon riveted PtRu/C catalyst electrodes were used as the working electrode. The catalyst ink was prepared by ultrasonically dispersing catalyst powders in an appropriate amount of ultrapure water. The catalyst ink of 5 μL was dropped onto a glassy carbon working electrode, and was dried for 15 min. Later, 5 μL of Nafion solution (5 wt. %) was spread on the surface of electrode, and dried in air. In all cases, the total loading of metal was 28 μg cm^{-2}.

The electrochemical measurements of the catalysts were carried out in a glass sealed cell containing 0.5 mol L^{-1} H_2SO_4 and 0.5 mol L^{-1} CH_3OH solutions at 25 ± 1^{o}C. Highly purified argon gas was purged into the solution for 20 min to eliminate oxygen.

The stability of the catalyst was evaluated by the accelerated potential cycling test (APCT) which was conducted within the potential range of 0.05–1.20 V (versus RHE) with a scanning rate of 50 mV s^{-1}. All potentials are reported with respect to reversible hydrogen electrode in this paper.

The electroactive specific surface area of PtRu/C catalyst was determined by CO_{ad} stripping voltammetry, assuming the formation of a monolayer of linearly adsorbed CO and the coulombic charge required for oxidation of CO_{ad} to be 420 mC cm^{-2}. The voltammetry was carried out in 0.5 mol L^{-1} H_2SO_4 at 25°C with a scanning rate of 50 mV s^{-1}.

The electrochemical tests of these MEAs were carried out by Fuel Cell Testing System (Scribner Associates Inc., Series 890E, Southern Pines, NC, USA) using the single cell (Electrochemistry Corp.). The methanol solution of 1.5 mol L^{-1} was fed to the anode side with a flow rate of 3.0 mL min^{-1}. Pure oxygen was supplied to the cathode side with a flow rate of 200 mL min^{-1} under ambient pressure. The cell was operated at 80 °C. The polarization curves and power density curves of the MEAs were plotted at intervals of operating time. Each point on the polarization curves and power density curves represented a steady-state performance achieved after about 3 min of continuous operation at a given voltage. Potential–time curves of the two single cells were plotted in a galvanostatic mode with a current density of 150 mA cm^{-2} for 100 h. To ensure the electrolyte in the Nafion membrane and MEA electrode is moist enough to have high ionic conductivity, it is necessary to activate the MEA before the performance measurements. In our experiment, the single cells were conditioned with ultrapure water and oxygen at 80 °C for 5 h. And then, ultrapure water was replaced with methanol solution of 1.5 mol L^{-1} for 20 h in a galvanostatic mode with a current density of 30 mA cm^{-2} prior to the acquisition of life data.

3. Results and discussion

Scheme 1 shows the fundamental of glucose in-situ carbonization through hydrothermal method (GICH). Specifically, the mean size of the as-prepared PtRu nanoparticles grows remarkable because of the coalescence by its migration on the support surface during the accelerated potential cycling test (APCT). However, that of the carbon riveted PtRu nanoparticles grows slightly, which is because the existence of carbon nanolayer on surface of

the support from glucose in-situ carbonization inhibits the migration and coalescence of PtRu nanoparticles on the support.

For the sake of convenience, the as-prepared PtRu/C catalyst is designated as S-0. Carbon riveted PtRu/C catalysts prepared in different hydrothermal treatment time of 3, 4, and 5h are designated as S-3h, S-4h and S-5h, respectively. Carbon riveted PtRu/C catalysts prepared with coating amount of 0%, 9%, and 12% are designated as S-0%, S-9%, and S-12%. In addition, the coating amount of S-3h, S-4h, and S-5h catalysts is 6%. The hydrothermal treatment time of S-0%, S-9% and S-12% is the optimized time of 4 h.

Scheme 1

3.1 Effect of hydrothermal treatment time on the performance of PtRu/C catalyst

Firstly, we exactly investigate the effect of hydrothermal treatment time on performance of carbon riveted PtRu/C catalyst. Fig. 1 shows the XRD patterns of S-0, S-3h, S-4h, and S-5h catalysts, respectively. The diffraction peaks at 26^{o} can be attributed to the hexagonal graphite structures (002) of the carbon black. Besides, the 2θ values of the other four peaks correspond to the (111), (200), (220), and (311) crystal planes of crystalline face-centered cubic PtRu, and it also can be obviously seen the crystallinity of PtRu nanoparticles increase with the hydrothermal treatment time.

Fig. 1

TEM images with associated size distributions of S-0, S-3h, S-4h, and S-5h catalysts before and after APCT are shown in Fig. 2. More intuitive mean sizes of all samples are provided in Table 1. It can be clearly seen from Fig. 2 that the as-prepared PtRu nanoparticles (S-0)

deposit on XC-72 surface uniformly. With the increasing of hydrothermal time, the PtRu nanoparticles appear aggregation to some extents. When hydrothermal time is 5 h, the coalescence of PtRu particles becomes the most serious, that can be clearly seen from Fig. 2 (D-1, 2). Definitely, the mean sizes of PtRu nanoparticles of S-3h, S-4h, and S-5h catalysts increase from initial 2.1 to 2.3, 2.7, and 3.5 nm, respectively. It is reasonable that the coalescence of metal particles becomes seriously with the prolonging of hydrothermal time. With regard to the TEM images after APCT, the mean sizes of S-0, S-3h, S-4h, and S-5h grow to 3.8, 3.1, 3.1 and 3.8 nm, increasing by 81%, 35%, 15%, and 10% in comparison with that before APCT, respectively. Thus the process in Scheme 1 effectively anchors the crystallites and inhibits migration and agglomeration (coalescence) of the PtRu nanoparticles. The results of TEM are in accord with the results of electrochemical measurements discussed below.

Fig. 2

Table 1

The long-time stability behavior of S-0, S-3h, S-4h, and S-5h catalysts toward methanol electro-oxidation are investigated by the continued CV cycles as previously reported [37] and the normalized peak current densities are presented in Fig. 3. It is particularly informative that S-0 has a sharp decline at 200 cycles and decays nearly 45% of its activity at 1000 cycles, comparing the 40%, 22%, and 17% for S-3h, S-4h, and S-5h, respectively. The sharp decline during 200 cycles may be because of the dissolution of Ru at high potential leading a weak CO tolerance.[38, 39] Compared with as-prepared PtRu/C, the carbon riveted PtRu/C catalysts (S-3h, S-4h, and S-5h) show the ultrahigh stability. In addition, the methanol catalytic activity of S-3h and S-4h does not changed drastically compared with S-0 before the accelerated potential cycling test. In addition, the activity of S-5h catalyst becomes practically constant

after nearly 200 cycles. This behavior could be because of its largest size of metal particles, which about 3.5 nm before the accelerated potential cycling test (APCT), among all the samples. This size even is larger than that of S-3h and S-4h after APTC. Undoubtedly, the larger size of catalyst particles has a higher stability. On the other hand, the initial activity of S-5h catalyst is much lower than other catalysts leading an unobvious activity loss. We consider that the shortage of the hydrothermal time (S-3h) leads to the incompletion of glucose carbonized. However, when the hydrothermal time is too long (S-5h), the large size of the PtRu nanoparticles will result a low catalytic activity. Combining with the results of Fig. 2, the CV results further demonstrate that the carbon riveted PtRu/C catalysts treated for 4 h has the best performance for methanol electrooxidation.

Fig. 3

3.2 Effect of coating amount on the performance of PtRu/C catalyst

In this section, the effect of coating amount on the performance of PtRu/C catalyst is further investigated. Fig.4 shows the XRD patterns of carbon riveted catalysts (S-0%, S-4h, S-9%, and S-12%) with different coating amounts of 0%, 6%, 9%, and 12% (values are calculated before hydrothermal treatment), respectively. It can be obviously seen from Fig.4 that the crystallinity of the PtRu nanoparticles decreases with the increasing of carbon coating amount. This possibly because of the carbon nanolayer on the surface of catalyst, which can cover the metal particles to some extent, becomes thicker as the carbon coating amount increasing.

Fig. 4

TEM images with associated size distributions of S-0%, S-9%, and S-12% catalysts before and after APCT are shown in Fig. 5. After the same hydrothermal treatment of 4 h, S-0%, S-4h, S-9% and S-12% catalysts have the similar nanoparticles size of 2.7 nm. With regard to the TEM images after APCT, it can be obviously seen that the mean sizes of three carbon riveted PtRu/C catalysts (S-4h, S-9% and S-12%) grow to 3.1, 3.0 and 3.1 nm, respectively. However, the mean sizes of non-carbon riveted PtRu/C (S-0%) nanoparticles grow from the initial size of 2.7 nm to 4.0 nm. The smaller size growth of three carbon riveted PtRu/C catalysts is because of the riveted carbon layer formed during the hydrothermal treatment effectively anchors the crystallites and inhibits migration and agglomeration (coalescence) of the PtRu nanoparticles during the APCT. In addition, though S-12% has the smaller size after APCT, but it shows the bad performance for methanol electro-oxidation. The reason for this abnormal phenomenon can be found out in Fig.6.

Fig. 5

Fig. 6 shows HRTEM images of S-0%, S-4h, S-9%, and S-12% before APCT. The carbonized carbon layers about 2.0, 3.5 and 5.1 nm for S-4h, S-9%, and S-12% can be clearly observed from those images, respectively. While, no obviously carbon layers can be seen in Fig. 6a for S-0% sample. It is not surprise that the carbon layers become thicker with the increasing of coating amount. Combining with the results of CV from Fig. 7, S-9% catalyst with the carbonized carbon layer of 3.5 nm has the best performance. For S-12% catalyst, the thicker carbonized carbon layers seriously cover the PtRu metal nanoparticles, which lead to the lower catalytic activity. In addition, because of the similar catalytic activity of S-0%, S-4h, and S-9%, it can confirm that the porous carbonized carbon layers on surface of the catalyst slightly cover the metal catalytic active sites.

Fig. 6

The fact of the porous carbonized carbon layer slightly covered the active sites also can be confirmed from the CO_{ad} stripping voltammograms as shown in Fig. 7. The electrochemical active specific surface areas (ESA) of S-0 and S-9% calculated by CO_{ad} stripping voltammetry are 89.1 and 86.3 m^2 g^{-1} Pt, respectively. The slightly decreased ESA is due to the existent of porous carbon layer covering the active sites. The onset potential for oxidation of adsorbed CO on S-9% catalyst shift to a lower electrode potential by 47.0 mV compared with the as-prepared PtRu/C. The negative potential shift should originate from the facts that the size of PtRu nanoparticles increases[40] and the surface ratio of Pt and Ru is more appropriated for electrooxidation of adsorbed CO molecules on carbon riveted PtRu/C catalyst after hydrothermal treatment.

Fig. 7

Fig. 8 shows the long-time stability behavior of carbon riveted catalysts with different coating amounts of 0%, 6%, 9%, and 12% and their normalized peak current densities. After 1000 APTC, S-0% catalyst has a current density decline of 27.0%, comparing with the 22.0%, 19.8%, and 17.2% for S-4h, S-9%, and S-12%, respectively. As the carbon coating amount increasing, the stability of those catalysts gradually enhances. Obviously, S-9% with the carbon coating amount of 9% shows the best catalytic activity and stability. Compared with the 44.3% current density decrement of S-0 as shown in Fig. 3, which of the S-9% with the similar activity is only 19.8% after APCT of 1000 cycles. Therefore, 9% is the optimal carbon coating amount in our experimental conditions.

Fig. 8

Deconvoluted Pt 4f, Ru 3p, C 1s, and O 1s peaks from XPS analysis of S-0 and S-9% catalysts are shown in Fig. 9. The curves fitting of Pt 4f, Ru 3p, C 1s, and O 1s peaks of the X-ray photoelectron spectra for S-0 and S-9% catalysts are in accordance with our previous work.[33] The binding energies of all components along with their relative intensities are provided in Table 2, Table 3, Table 4, and Table 5, respectively. Not surprisingly, the content of Pt(0) increases by 12.53% accompanied with decreasing by 9.11% of Pt(II), demonstrating that the carbon riveted PtRu/C catalyst has the higher stability relative to as-prepared PtRu/C catalyst due to more corrosion resistance of Pt(0).[41] Consistent with the results of Pt 4f, the content of Ru(0) increases from 21.99% to 39.66% after glucose in-situ carbonization. The increased metallic Pt and Ru content of S-9% sample can be attributed to the stronger reducibility of glucose at high temperature. The XPS results of C1s spectra show that the relative intensities of oxygen containing functional groups of carbon riveted PtRu/C catalyst are higher than that of as-prepared PtRu/C. The oxygen containing functional groups, formed from the carbonization of glucose, can effectively anchor and stabilize the metal NPs in situ.[42] Furthermore, it is also clearly seen in Table 3 that the sp^3 C in carbon riveted PtRu/C catalyst is 8.49% greater than that in as-prepared PtRu/C, indicating the carbon from carbonization of glucose has higher stability than XC-72 carbon black. This may be another reason for the ultrahigh stability of the carbon riveted PtRu/C catalyst.

Fig. 9

Table 2

Table 3

Table 4

Table 5

In order to testify the stability of carbon riveted catalyst practically, the life tests of two single cells, which separately used as-prepared 40 wt. % PtRu/C and carbon riveted 40 wt. % PtRu/C as anode catalysts, are carried out at a cell temperature of 80^{o}C at a high current density of 150 mA cm^{-2}. As shown in Fig. 10 a, the majority of voltage losses occur in the first few hours and then their decay become less significant. The initial rapid performance loss is attributed to the non-equilibrium state among ruthenium oxides. During the whole life test, the cell voltages decrease with test time, there is a slow performance loss that is irrecoverable, which might relate to the degradation of catalysts, the dissolution of Nafion® solution in the catalyst layers, and the aging of polymer electrolyte membrane. For two single fuel cells, excepted for the difference of anode catalyst, other parts are totally the same. Therefore, the performance loss of both can directly reflect the stability of two catalysts. Compared with the voltage decay of 82.9 mV for the reference DMFC used as-prepared PtRu/C catalyst, which of the carbon riveted PtRu/C is only about 30.0 mV after a constant current life test of 100 h. The carbon riveted catalyst shows the higher stability.

Fig. 10

The cell performances before and after life test are compared by polarization and power density curves of the two single cells. The cell performances all have different extents of decay with test time. Their maximum power densities (MPD) before life test are similar, about 73.2 and 76.6 mW cm^{-2} for as-prepared and carbon riveted catalysts, respectively. For the cell used as-prepared catalyst as shown in Fig. 10 b, its MPD drops 28.4% after a test time of 100

h. While at the same conditions, the DMFC used carbon riveted PtRu/C as anode catalyst in Fig. 10 c shows the better stability with a less MPD drop of 12.0%. Furthermore, its loss of power density at a cell voltage of 0.4 V is also lesser than that of the reference DMFC, about 6.9 and 32.3% for as-prepared and carbon riveted catalysts, respectively.

4. Conclusions

In summary, the carbonized carbon layer about 2-5nm is successfully coated on the surface of the as-prepared PtRu/C catalyst. The optimal hydrothermal treatment time is 4 h. Shortage of the hydrothermal time leads to the incompletion of glucose carbonized. While, when the hydrothermal time is too long, the large size of the PtRu nanoparticles will result a bad catalytic activity. When the carbon coating amount is 9%, the carbon riveted PtRu/C catalyst with a 3.5 nm carbonized carbon layer has the best performance. The accelerated potential cycling test and the life test of single cell all show the carbon riveted PtRu/C catalyst prepared for 4 h and carbon coating amount of 9% has higher stability with a similar initial activity as compared to the as-prepared PtRu/C. After 100 h life test, the maximum power density of single fuel cell that used the carbon riveted PtRu/C as anode catalyst drops only 12.0% from 76.6 to 67.4 mW cm^{-2}, comparing the 28.4% from 73.2 to 52.4 mW cm^{-2} for as-prepared PtRu/C. And the voltage decay of 82.9 mV for the DMFC used as-prepared PtRu/C catalyst is almost two times higher than that of about 30.0 mV decay used the carbon riveted PtRu/C after constant current life test of 100 h. The significantly enhanced stability for carbon riveted PtRu/C catalyst is attributed to two critical reasons: (1) the anchoring effect of carbon nanolayer formed during the glucose in-situ carbonization through hydrothermal method; (2) the content increasing of Pt (0), Ru(0), sp^3 hybridization carbon and C-OR groups composition and the evidently decreasing PtO_2 and RuO_xH_y after the carbon riveted process.

Acknowledgements

This research is financially supported by the National Natural Science Foundation of China (Grant No. 21273058), China postdoctoral science foundation (Grant No.2012M520731 and 2014T70350), Heilongjiang postdoctoral foundation (LBH-Z12089) and outstanding subject leaders of special fund project of Harbin in China (Grant No.2012RFXXG99).

References

1 Z. Wang, G. Shi, J. Xia, F. Zhang, Y. Xia, Y. Li, L. Xia, *Acta Chim. Sinica*, 2013, **71**, 1225-1238.

2 S. Sharma, B.G. Pollet, *J. Power Sources*, 2012, **208**, 96-119.

3 M.K. Debe, *Nature*, 2012, **486**, 43-51.

4 X. Zhao, M. Yin, L. Ma, L. Liang, C. Liu, J. Liao, T. Lu, W. Xing, *Energy Environ. Sci.*, 2011, **4**, 2736-2753.

5 L. La-Torre-Riveros, R. Guzman-Blas, A.E. Mendez-Torres, M. Prelas, D.A. Tryk, C.R. Cabrera, *ACS Appl. Mater. Interfaces*, 2012, **4**, 1134-1147.

6 Y. Okawa, T. Masuda, H. Uehara, D. Matsumura, K. Tamura, Y. Nishihata, K. Uosaki, *RSC Adv.*, 2013, **3**, 15094.

7 X.F. Yu, D.S. Wang, Q. Peng, Y.D. Li, *Chem. Eur. J.*, 2013, **19**, 233-239.

8 A. Santasalo-Aarnio, M. Borghei, I.V. Anoshkin, A.G. Nasibulin, E.I. Kauppinen, V. Ruiz, T. Kallio, *Int. J. Hydrogen Energy*, 2012, **37**, 3415-3424.

9 X.L. Yang, X.Z. Liu, X.Y. Meng, X.Y. Wang, G. Li, C.Y. Shu, L. Jiang, C.R. Wang, *J. Power Sources*, 2013, **240**, 536-543.

10 A.Y. Lo, N.Y. Yu, S.J. Huang, C.T. Hung, S.H. Liu, Z.B. Lei, C.T. Kuo, S.B. Liu, *Diamond Relat. Mater.*, 2011, **20**, 343-350.

11 D.P. He, C. Zeng, C. Xu, N.C. Cheng, H.G. Li, S.C. Mu, M. Pan, *Langmuir*, 2011, **27**, 5582-5588.

12 L. Jiang, H. Fu, L. Wang, W. Zhou, B. Jiang, R. Wang, *RSC Adv.*, 2014, **4**, 51272-51279.

13 S. Kang, S. Lim, D.H. Peck, S.K. Kim, D.H. Jung, S.H. Hong, H.G. Jung, Y. Shul, *Int. J. Hydrogen Energy*, 2012, **37**, 4685-4693.

14 K. Kakaei, M. Zhiani, *J. Power Sources*, 2013, **225**, 356-363.

15 K. Ji, G. Chang, M. Oyama, X.Z. Shang, X. Liu, Y.B. He, *Electrochim. Acta*, 2012, **85**, 84-89.

16 D. Bin, F. Ren, H. Wang, K. Zhang, B. Yang, C. Zhai, M. Zhu, P. Yang, Y. Du, *RSC Adv.*, 2014, **4**, 39612-39618.

17 W. Wang, H. Wang, J. Key, V. Linkov, S. Ji, R.F. Wang, *Ionics*, 2013, **19**, 529-534.

18 K.W. Park, Y.W. Lee, J.K. Oh, D.Y. Kim, S.B. Han, A.R. Ko, S.J. Kim, H.S. Kim, *J. Ind. Eng. Chem.*, 2011, **17**, 696-699.

19 H. Chhina, S. Campbell, O. Kesler, *J. Power Sources*, 2006, **161**, 893-900.

20 T. Zhu, C.Y. Du, C.T. Liu, G.P. Yin, P.F. Shi, *Appl. Surf. Sci.*, 2011, **257**, 2371-2376.

21 Y. Zhou, W.M. Liu, X.C. Hu, Y.Q. Chu, C.A. Ma, *Acta Phys.-Chim. Sin.*, 2013, **29**, 1487-1493.

22 Y. Zhou, Y.Q. Chu, W.M. Liu, C.A. Ma, *Acta Phys.-Chim. Sin.*, 2013, **29**, 287-292.

23 F. Wu, Y.H. Liu, C. Wu, *Rare Metals*, 2010, **29**, 255-260.

24 A.T.E. Vilian, M. Rajkumar, S.-M. Chen, C.-C. Hu, K.M. Boopathi, C.-W. Chu, *RSC Adv.*, 2014, **4**, 41387-41397.

25 H. Huang, S. Yang, R. Vajtai, X. Wang, P.M. Ajayan, *Adv Mater*, 2014, **26**, 5160-5165.

26 M. Kim, S. Hwang, J.S. Yu, *J. Mater. Chem.*, 2007, **17**, 1656-1659.

27 C.-Z. Li, Z.-B. Wang, X.-L. Sui, L.-M. Zhang, D.-M. Gu, S. Gu, *J. Mater. Chem. A*, 2014, DOI: 10.1039/C4TA04594G.

28 A.Y. Lo, C.T. Hung, N.Y. Yu, C.T. Kuo, S.B. Liu, *Applied Energy*, 2012, **100**, 66-74.

29 S. Takenaka, H. Matsumori, H. Matsune, E. Tanabe, M. Kishida, *J. Electrochem. Soc.*, 2008, **155**, B929-B936.

30 B.Y. Xia, S. Ding, H.B. Wu, X. Wang, X. Wen, *RSC Adv.*, 2012, **2**, 792-796.

31 T. Fujigaya, N. Nakashima, *Adv. Mater.*, 2013, **25**, 1666-1681.

32 C. Zhou, F. Peng, H. Wang, H. Yu, C. Peng, J. Yang, *Electrochem. Commun.*, 2010, **12**, 1210-1213.

33 Z.Z. Jiang, Z.B. Wang, D.M. Gu, E.S. Smotkin, *Chem. Commun. (Camb)*, 2010, **46**, 6998-7000.

34 Z.-Z. Jiang, Z.-B. Wang, Y.-Y. Chu, D.-M. Gu, G.-P. Yin, *Energy Environ. Sci.*, 2011, **4**, 728-735.

35 Z.-Z. Jiang, Z.-B. Wang, Y.-Y. Chu, D.-M. Gu, G.-P. Yin, *Energy Environ. Sci.*, 2011, **4**, 2558-2566.

36 Z.Z. Jiang, Z.B. Wang, W.L. Qu, H. Rivera, D.M. Gu, G.P. Yin, *Nanoscale*, 2012, **4**, 7411-7418.

37 Z.-B. Wang, C.-Z. Li, D.-M. Gu, G.-P. Yin, *J. Power Sources*, 2013, **238**, 283-289.

38 K. Matsuoka, S. Sakamoto, A. Fukunaga, *J. Power Sources*, 2013, **238**, 251-256.

39 Y. Sugawara, A.P. Yadav, A. Nishikata, T. Tsuru, *J. Electrochem. Soc.*, 2008, **155**, B897.

40 T. Saida, W. Sugimoto, Y. Takasu, *Electrochim. Acta*, 2010, **55**, 857-864.

41 W. Li, A.M. Lane, *Electrochem. Commun.*, 2009, **11**, 1187-1190.

42 Y.J. Kuang, Y. Cui, Y.S. Zhang, Y.M. Yu, X.H. Zhang, J.H. Chen, *Chem. Eur. J.*, 2012, **18**, 1522-1527.

List of figures and tables

40 wt. % PtRu/C, metal loading 2.5 mg cm^{-2}. Cathodic catalyst: 40 wt. % Pt/C, metal loading 2.5 mg cm^{-2}. b) Performances of single DMFC used as-prepared 40 wt. % PtRu/C before and after different test times. c) Performances of single DMFC used carbon riveted 40 wt. % PtRu/C before and after different test times. Operating conditions: 80°C, 150 mA cm^{-2}. Anodic feed: 1.5 mol L^{-1} CH_3OH solution with a flow rate of 3.0 mL min^{-1}. Cathodic feed: oxygen at ambient pressure with a flow rate of 200 mL min^{-1}.

Table 1 Mean sizes of different PtRu/C catalysts

Table 2 Results of the fits of the Pt4f spectra

Table 3 Results of the fits of the Ru3p spectra

Table 4 Results of the fits of the C1s spectra

Table 5 Results of the fits of the O1s spectra

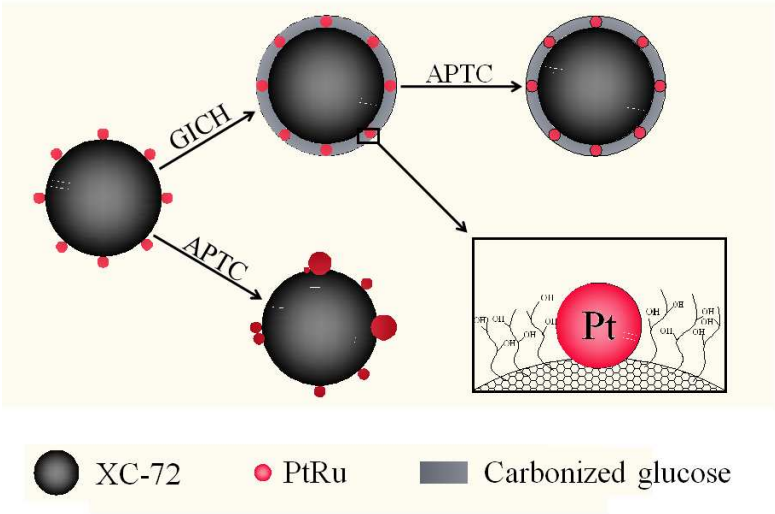

Scheme 1

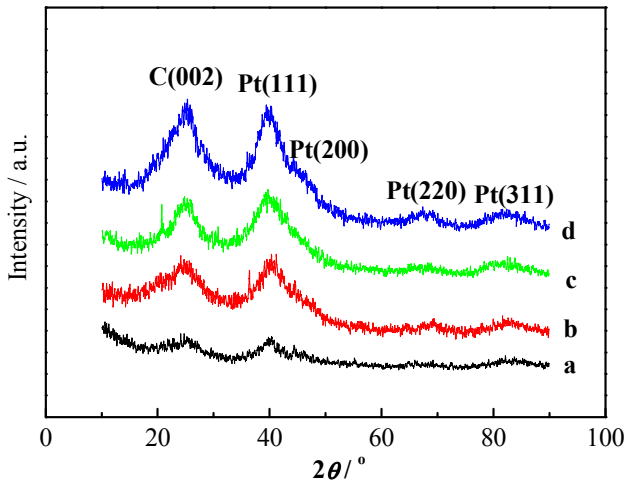

Fig. 1

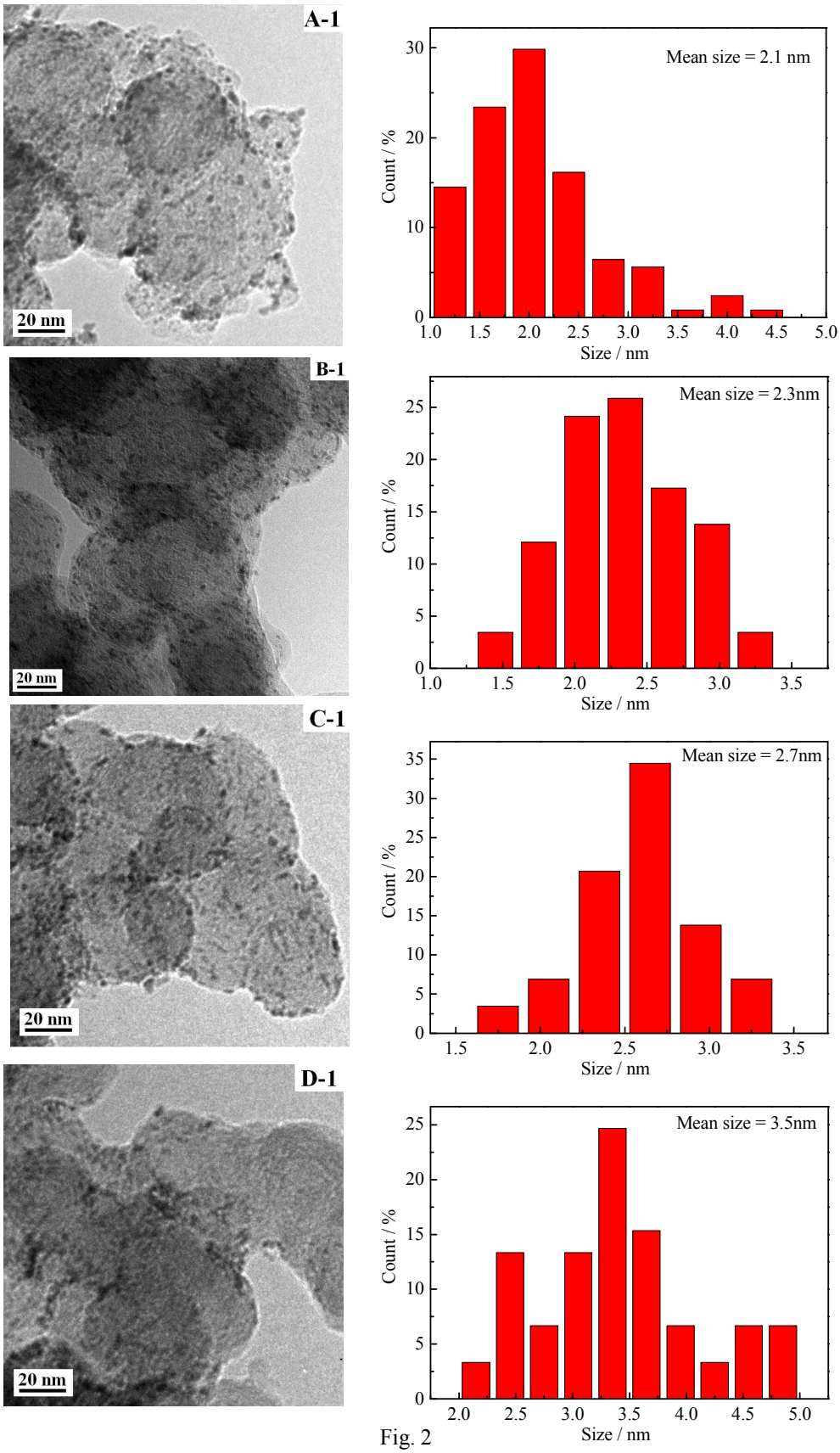

Fig. 2

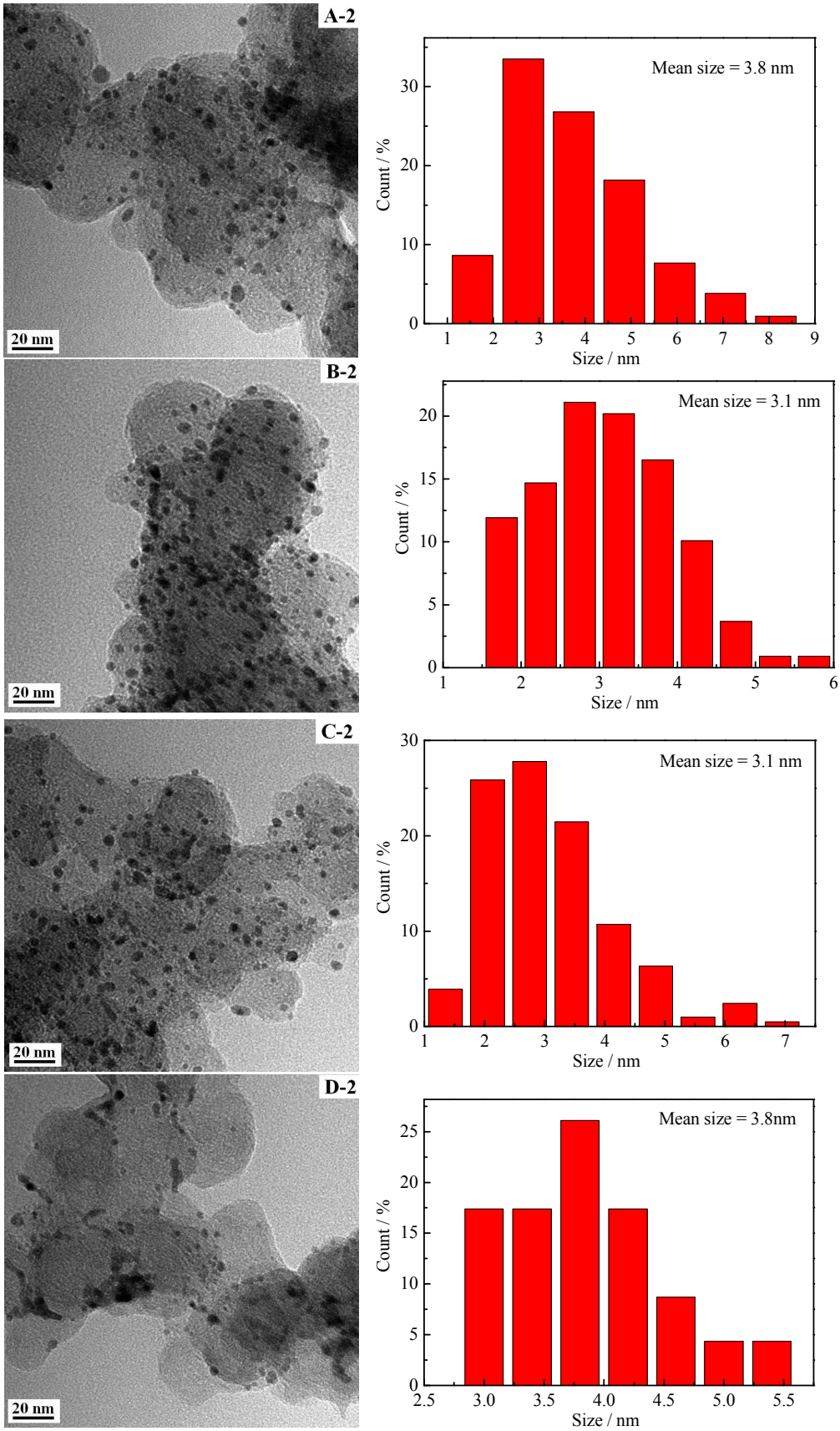

Fig. 2 (Continued)

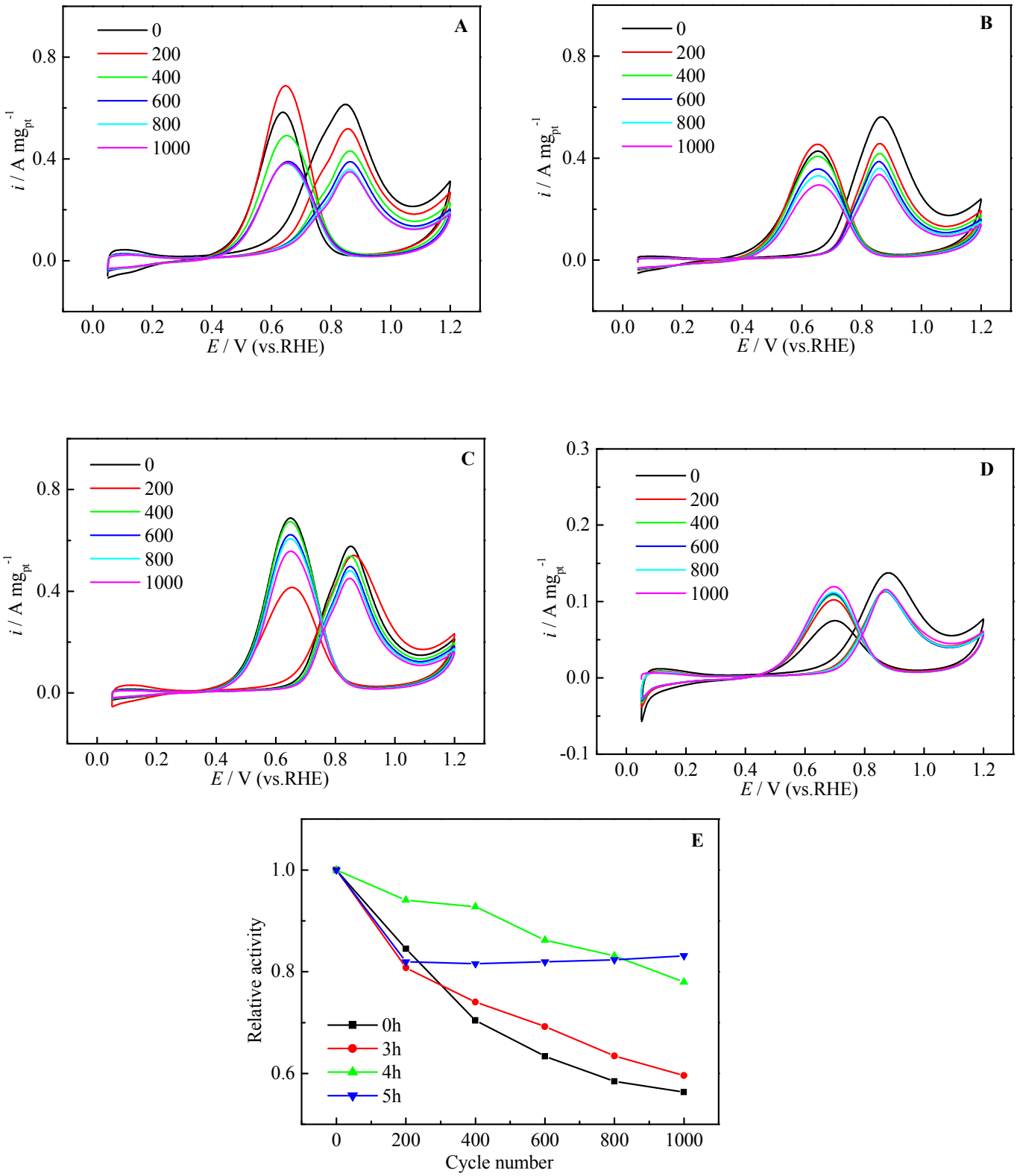

Fig. 3

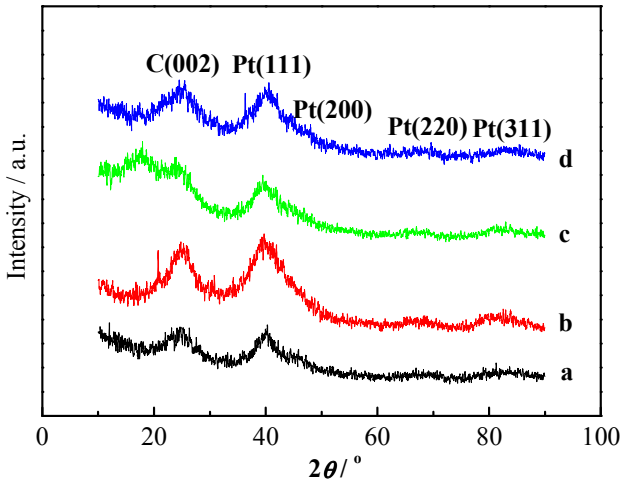

Fig. 4

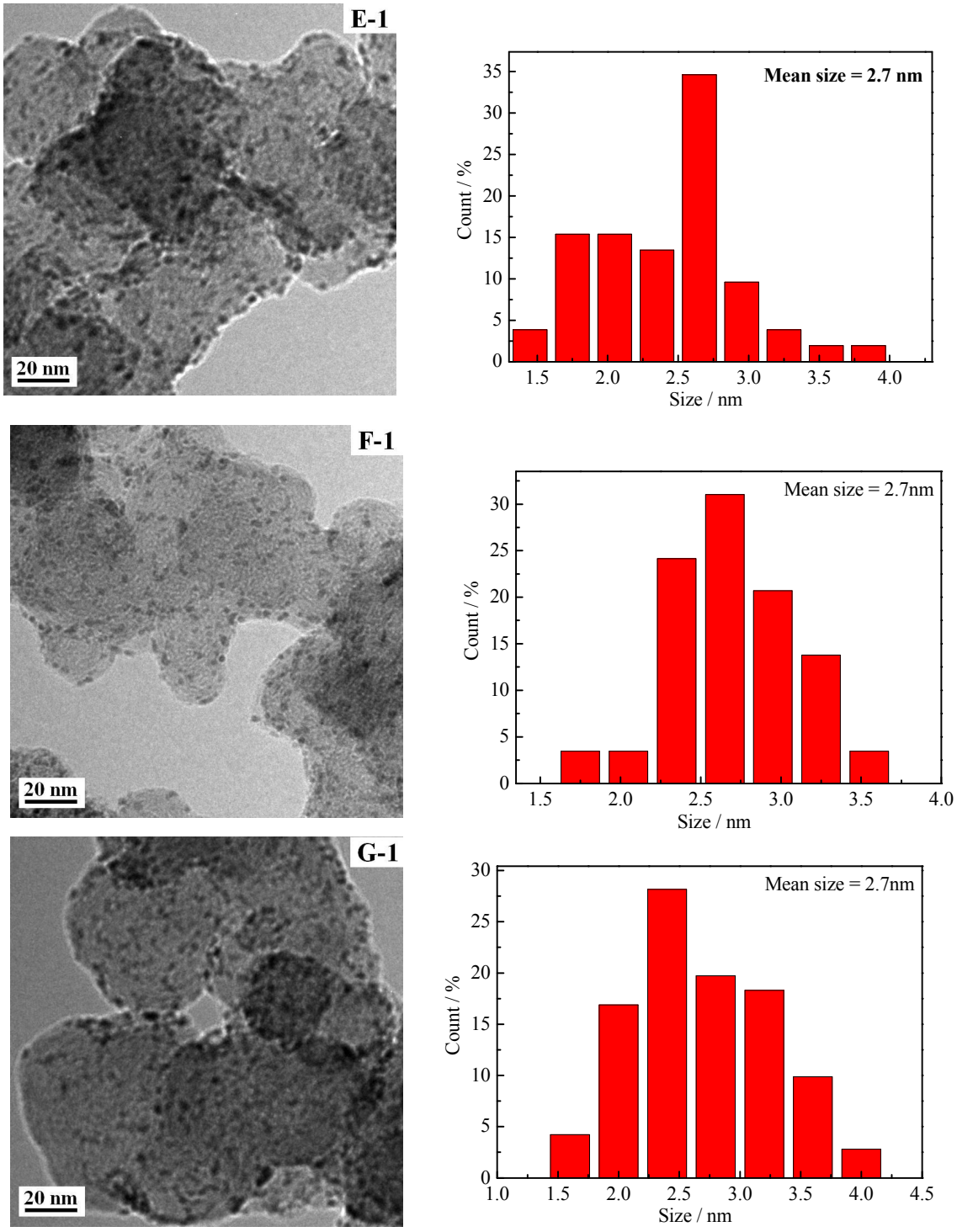

Fig. 5

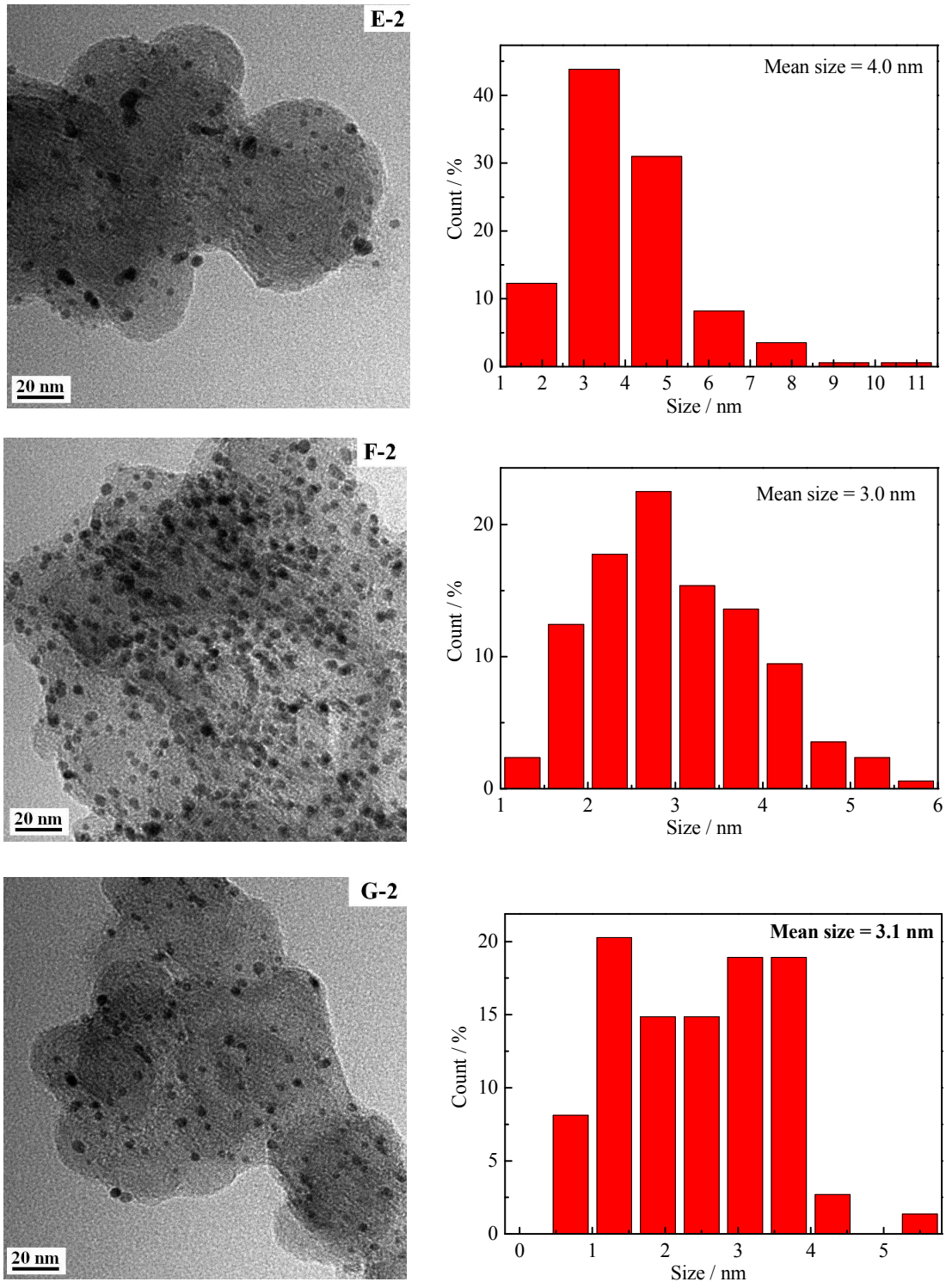

Fig. 5 (Continued)

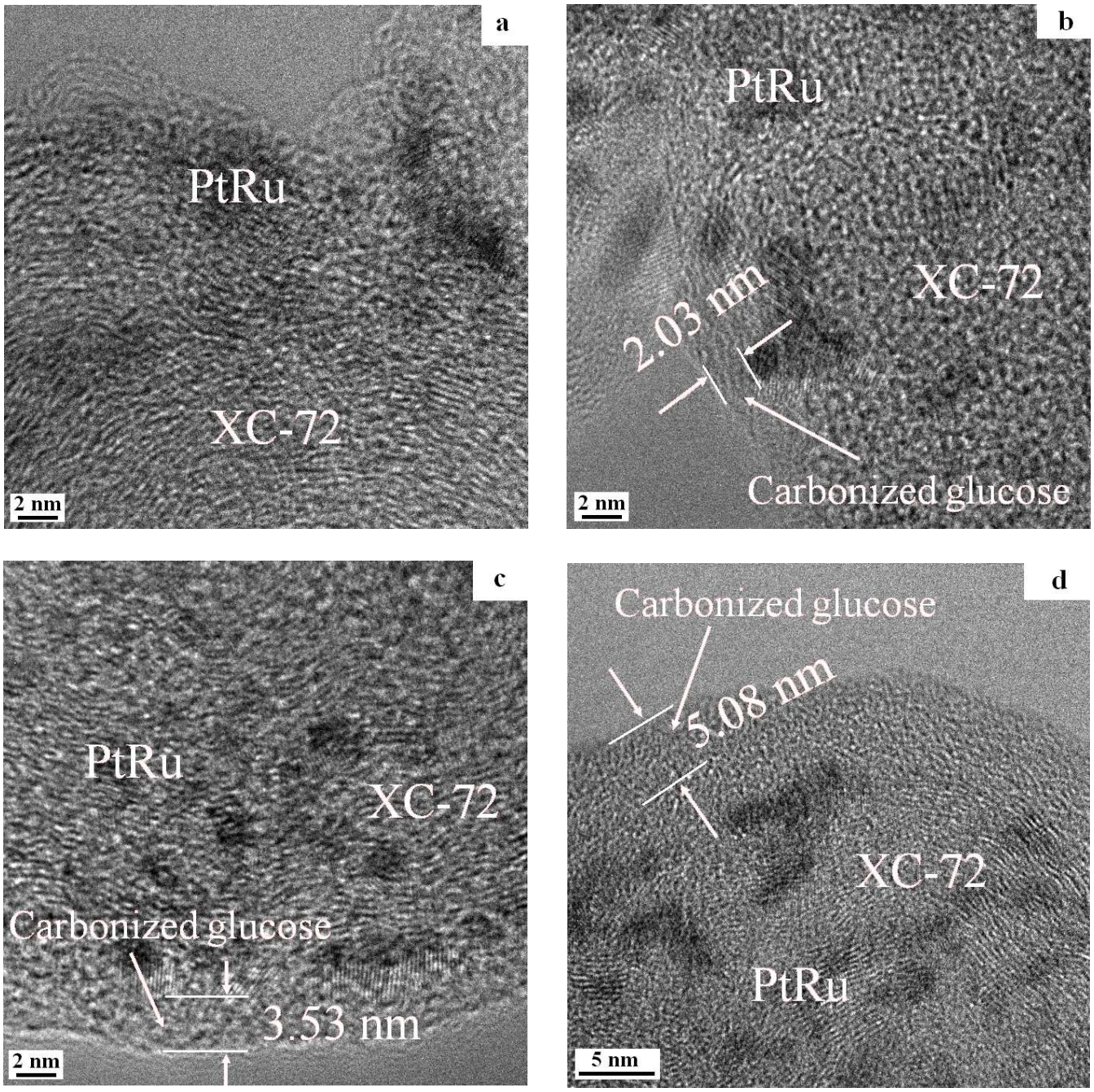

Fig. 6

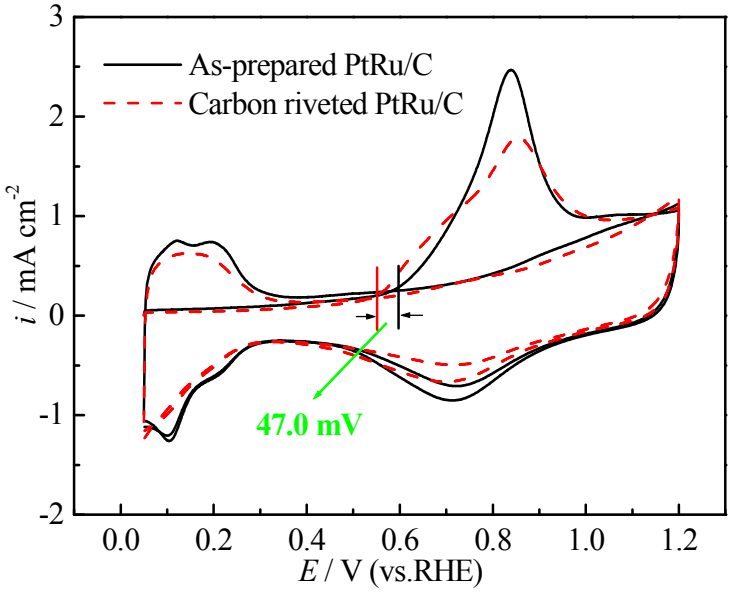

Fig. 7

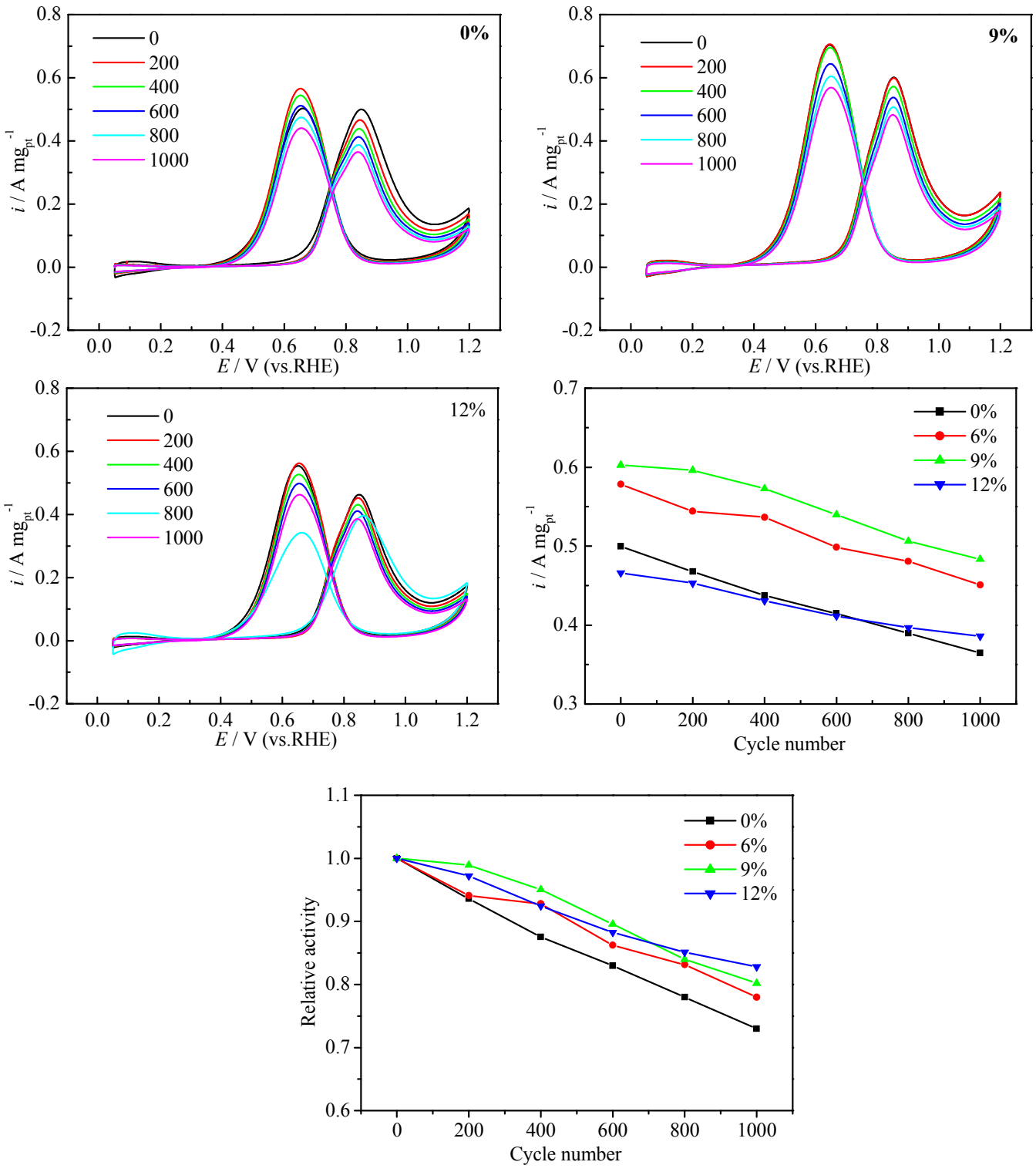

Fig. 8

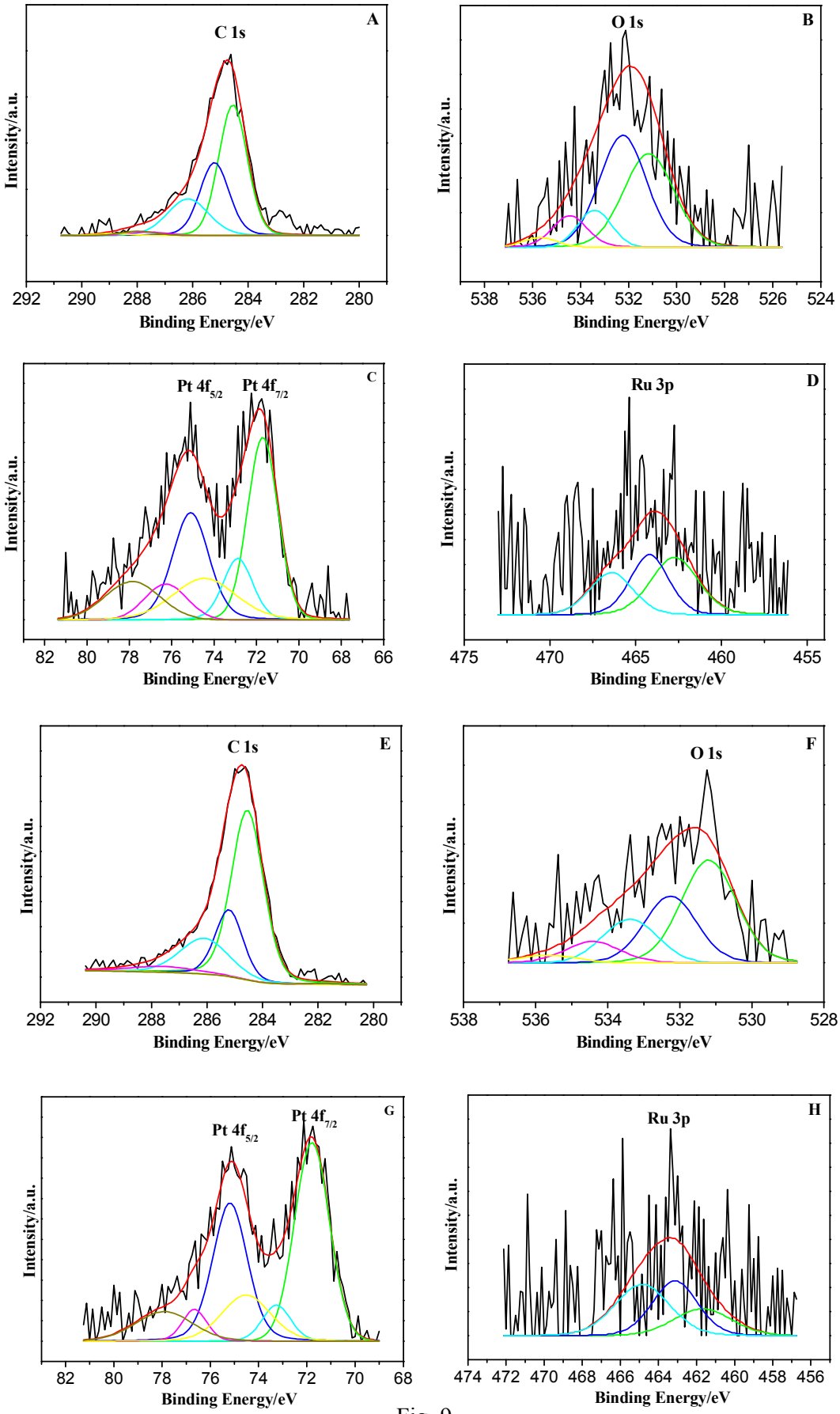

Fig. 9

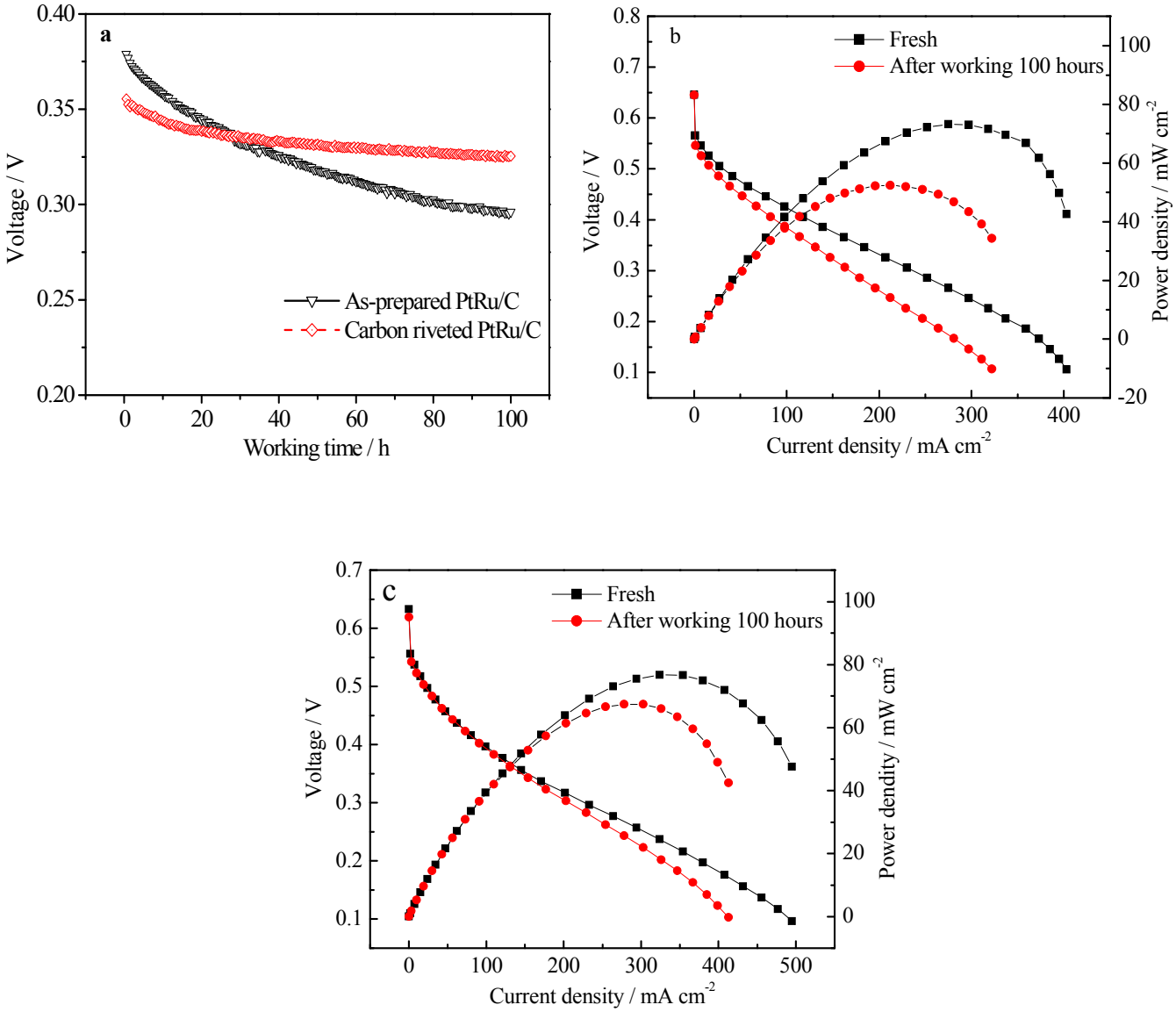

Fig. 10

Table 1

Sample	S-0 (A-1,2)	S-3h (B-1,2)	S-4h (C-1,2)	S-5h (D-1,2)	S-0% (E-1,2)	S-9% (F-1,2)	S-12% (G-1,2)
Sizes before treatment (nm)	2.1	2.3	2.7	3.5	2.7	2.7	2.7
Sizes after treatment (nm)	3.8	3.1	3.1	3.8	4.0	3.0	3.1

Table 2

Catalysts	Species	Orbital spin	Binding energy/eV	Peak half width/eV	Assignment	Relative content/%
As-prepared PtRu/C	Pt 4f	$4f_{7/2}$	71.71	1.69	Pt	30.95
		$4f_{5/2}$	75.11	2.02	Pt	23.02
		$4f_{7/2}$	72.88	1.64	PtO	10.85
		$4f_{5/2}$	76.28	2.35	PtO	8.20
		$4f_{7/2}$	74.46	3.50	PtO_2	15.61
		$4f_{5/2}$	77.86	3.08	PtO_2	11.38
Riveted PtRu/C	Pt 4f	$4f_{7/2}$	71.79	1.71	Pt	38.11
		$4f_{5/2}$	75.19	1.69	Pt	28.39
		$4f_{7/2}$	73.25	1.38	PtO	5.88
		$4f_{5/2}$	76.65	1.19	PtO	4.60
		$4f_{7/2}$	74.52	2.37	PtO_2	13.30
		$4f_{5/2}$	77.92	2.81	PtO_2	9.72

Table 3

Catalysts	Species	Orbital spin	Binding energy/eV	Peak half width/eV	Assignment	Relative content/%
As-prepared PtRu/C	Ru 3p	$3p_{1/2}$	461.68	3.60	Ru	21.79
		$3p_{1/2}$	463.33	2.80	RuO_2	43.59
		$3p_{1/2}$	464.85	3.40	RuO_xH_y	34.62
Riveted PtRu/C	Ru 3p	$3p_{1/2}$	462.73	3.00	Ru	39.66
		$3p_{1/2}$	464.19	2.64	RuO_2	33.62
		$3p_{1/2}$	466.42	3.25	RuO_xH_y	26.72

Table 4

Catalysts	Species	Bond	Binding energy /eV	Peak half width/eV	Relative content/%
As-prepared PtRu/C	C 1s	sp^2-C	284.54	1.36	57.46
		sp^3-C	285.20	1.18	19.98
		C-OR	286.10	2.02	18.07
		C=O	287.60	2.65	4.26
		COOR	288.74	1.73	0.22
		π	291.61	1.33	0
Riveted PtRu/C	C 1s	sp^2-C	284.55	1.21	47.84
		sp^3-C	285.22	1.24	28.47
		C-OR	286.17	1.76	19.59
		C=O	287.60	1.66	1.59
		COOR	287.97	1.40	1.71
		π	288.94	1.42	0.80

Table 5

Binding energy / eV	531.20 (-C=O)	532.26 (-OH)	533.39 (R-O-R)	534.42 (-COOH)	539.67 (H_2O)
As-prepared PtRu/C	43.61	27.07	17.29	9.02	3.10
Riveted PtRu/C	37.39	41.89	9.46	9.01	2.25